IEEE Access
Multidisciplinary | Rapid Review | Open Access Journal

IEEE ENGINEERING IN MEDICINE AND BIOLOGY SOCIETY SECTION

Received 18 November 2022, accepted 4 December 2022, date of publication 12 December 2022,
date of current version 21 December 2022.

Digital Object Identifier 10.1109/ACCESS.2022.3228479

RESEARCH ARTICLE

Bioimpedance Spectroscopy Helps Monitor the Impact of Electrical Stimulation on Muscle Cells

ALEXIA BAILLEUL[1], FLORENCE POULLETIER DE GANNES[1], ANTOINE PIROG[1], GILLES N'KAOUA[1], ADRIEN D'HOLLANDE[1], AURELIAN HOUE[1], FABIEN SOULIER[2], SERGE BERNARD[2], AND SYLVIE RENAUD[1]

[1]Univ. Bordeaux, CNRS, Bordeaux INP, IMS UMR 5218, 33405 Talence, France
[2]Univ. Montpellier, CNRS, LIRMM UMR 5506, 34095 Montpellier, France

Corresponding author: Sylvie Renaud (sylvie.renaud@ims-bordeaux.fr)

This work was supported in part by the Centre National de la Recherche Scientifique (SMARTSTIM Project, CNRS, France) under the PRIME'80 Program, and in part by the French Agence Nationale de la Recherche (ANR) under Agreement DIABLO N°ANR-18-CE17-0005-01.

ABSTRACT In this study, we present a first-of-a-kind biological-hardware-software tool to evaluate the physiological condition of in vitro myotubes in response to electrical stimulation. We demonstrate that impedance spectroscopy on a microelectrode array can testify for physiological changes of muscle cells under electrical stimulation. The platform is designed for simultaneous bioimpedance spectroscopy, electrical stimulation, and optical microscopy. It includes a microelectrode array, a custom hardware-software interface, and a commercial impedance analyzer. We used a well-established muscle cell model (C2C12) and developed a culture protocol suited for long-term recordings on microelectrode arrays. Electrical stimulation was applied with carbon electrodes and ad hoc electronics for current stimulation. Muscle cell bioimpedance measurement was complemented with optical microscopy video to record contractions. Then, the influence of electrical stimulation on the contractile activity of myotubes and on their bioimpedance was analyzed. Results validated the functionality of the hardware/software platform when used with our contractile muscle model. A bioimpedance-based metric was defined to evaluate changes in myotubes' physiology. After playing multiple stimulation scenarios, analysis showed that the bioimpedance metric decreases as duration or frequency of stimulation increase.

INDEX TERMS Bioimpedance, C2C12, electrical stimulation, electrophysiology, impedance spectroscopy, MEA, microelectrode array, myotubes, skeletal muscle.

I. INTRODUCTION

Understanding the key mechanisms behind muscle contraction is a challenging research topic with promising prospects in assessing the benefits of physical activity or the impact of muscle-based diseases. *In vivo* experiments – including skeletal muscle biopsies – constitute the most integrative models as they accurately reflect organ cross-talk and metabolism regulation. Still, *in vitro* models and technologies provide faithful alternatives and ethical research solutions to investigate the impact of exercise, injuries, and neuromuscular disorders on muscles [1], [2], [3].

The associate editor coordinating the review of this manuscript and approving it for publication was Kin Fong Lei.

During muscle contraction, biological phenomena occur, such as energy consumption (e.g. glucose, glycogen) and metabolites accumulation (e.g. lactate). Repeated or intense efforts lead to fatigue, which results in a decline in the contractile properties of the muscle: a decrease of the produced force, a decrease of the shortening speed, and the slowdown of the relaxation phase [4]. Muscle fatigue has mostly been investigated *in vivo* by various methods [5]: mechanical [6], metabolic [7], physiological [8], [9], electrical (e.g. electromyogram (EMG) [10] and electrical impedance myography (EIM) [11], [12], [13], [14]) measurements. *In vitro*, the fatigue effects of exercise are mainly quantified mechanically [15] and from a metabolic point of view [16], [17]. Estimation of fatigue through *in vitro* electrophysiological means is more

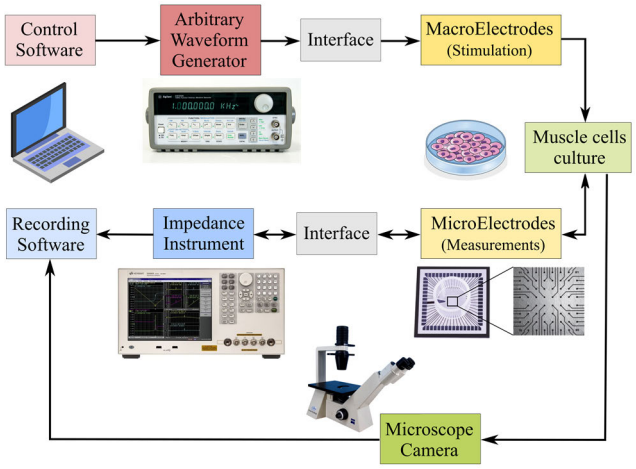

FIGURE 1. Schematic of the proposed setup including a stimulation system (composed of a programmable arbitrary waveform generator, a custom interface and carbon macroelectrodes) and a bioimpedance measurement system (comprising microelectrodes, an impedance analyzer and a custom interface). A PC allows both the control and the recording. Electrical stimulation and bioimpedance measurements are performed on in vitro muscle cell cultures.

complex than *in vivo* as it requires high-density microelectrodes array (MEA) to record the electrical activity of muscle cells and very complex signature analyses based on a large set of spike shapes [18]. Another possible electrical measurement is bioimpedance, which measures the passive electrical properties of tissues (conductive and dielectric properties [19]), often over a broad frequency range (bioimpedance spectroscopy). *In vitro* bioimpedance – developed by [20] – is a tool of growing interest, for the study of many metabolic and physiological changes in biological models at the cellular level, such as proliferation and differentiation [21], [22], [23], as well as atrophy and hypertrophy [24]. As it is already established that electrically stimulated muscle cells undergo morphological and metabolic changes [25], [26], [27], [28], we expect bioimpedance to be impacted by stimulation.

In this paper, we propose a new setup allowing the joint use of impedance spectroscopy and electrical stimulation of muscle cells, to recreate conditions for the occurrence of muscle fatigue *in vitro*. We present a proof of concept demonstrating that impedance spectroscopy on an MEA can testify for myotubes' physiological changes under electrical stimulation, and we discuss the relevance of computed metrics.

In [29], we presented an MEA-based setup for impedance spectroscopy of cultured muscle cells. This setup was enhanced as shown in Fig. 1 to feature controlled electrical stimulation and visual monitoring. By recreating controlled twitch or tetanic muscle contractions – quantified by image analysis – over long periods of time, we expect to identify a bioimpedance signature of muscle tissue fatigue.

Culturing techniques of skeletal myotubes from rodents and humans are relatively recent, and MEA technology is not common for skeletal muscle research and diagnostics. References [18], [30], and [31] performed the integration of primary skeletal muscle cells on MEA to investigate electrophysiological recordings (field potentials and action potential), without monitoring their bioimpedance. Conversely, [21], [22], [23] only implemented bioimpedance monitoring, using individual or interdigitated electrodes, in order to characterize myoblasts' growth and differentiation into myotubes. However, no studies to date combines both electrical stimulation and bioimpedance measurement on immortalized cell lines.

Furthermore, eliciting metabolic changes over a whole preparation requires large and controlled stimulation currents. Commercial systems performing both recordings and stimulations on MEA are essentially dimensioned to selectively process single cells organized in networks (neurons, cardiomyocytes) [30], [32] rather than whole preparations. Other commercial systems, using macroelectrodes, permit only voltage stimulation rather than current stimulation and have no microelectrodes for bioimpedance measurements [16], [17], [25], [26].

In this paper, we document the setup we designed for monitoring *in vitro* myotubes contractions. The system's functionality is validated by a series of experiments triggering different contraction types under stimulation. We propose a data processing method computing bioimpedance metrics and we analyze its relationships with stimulation patterns.

II. MATERIALS AND METHODS

We designed a full platform combining bioimpedance measurements, electrical stimulation and visual monitoring of cultured muscle cells (Fig. 1).

A. BIOIMPEDANCE MEASUREMENT SETUP

The bioimpedance measurement setup is based on the system described in [29], with some modifications.

The setup includes an MEA (MicroElectrodeDevices, Switzerland) with an array of 59 30-μm diameter Platinum-Black electrodes with 200-μm spacing and a SU-8 passivation layer. Impedance measurements are performed by a *Keysight E4990A* impedance analyzer (Keysight technologies, Santa Rosa, CA, USA). A custom holder and PCB were designed to interface the impedance analyzer to the MEA. The 3D printed holder features connectors and pogo pins (spring-loaded contacts) to immobilize and connect the MEA pad ring (Fig. 2). The PCB adapts the four BNC-connectors of the analyzer to a pair of wires that can be plugged into the connectors of the MEA holder.

Bioimpedance spectroscopy was made in a two-point configuration (between a pair of electrodes), in a frequency range from 100 Hz to 10 MHz with a 100 mV (peak-peak) sine wave, to cover frequency and impedance ranges relevant to physiology [19]. The setup allows to conduct two-point measurements on any pair of electrodes. All bioimpedance analyses in this paper were performed on the modulus response, although the phase was measured and computed as well.

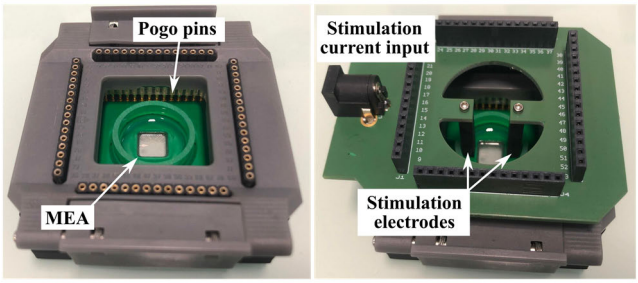

FIGURE 2. Left: Photograph of the custom MEA holder, which contacts the MEA pads through pogo-pins (spring-loaded contacts). Right: Photograph of the MEA holder topped with the stimulation PCB. Stimulation current is flowing between the two carbon electrodes.

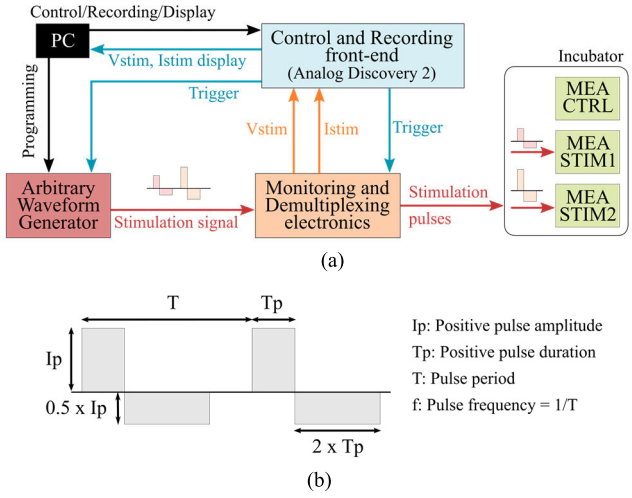

FIGURE 3. (a) Schematic of the stimulation system: the stimulation signal is generated by a programmable arbitrary waveform generator and delivered to 2 wells (MEAs) placed in an incubator. Signals travels through an interface allowing the demultiplexing of the pulses. A multifunction instrument (*Analog Discovery 2*) controls this interface and performs the acquisition of the stimulation current and voltage. A computer controls this instrument and the generator. (b) Parameters of a stimulation waveform composed of asymmetric biphasic pulses: Ip and Tp are the amplitude and duration of the positive pulse, T is the pulse period and f is the pulse frequency. Each positive pulse is balanced with a follow-up negative pulse (amplitude 0.5×Ip, duration 2×Tp) delivering the same quantity of opposite charge.

Prior to each experiment, MEAs were characterized before cell seeding with 1 mL of Phosphate-Buffered Saline (PBS). After the differentiation phase (see II-C), pairs of adjacent electrodes covered by visible and healthy myotubes were visually identified to be part of the set of electrodes pairs of interest. After the initial selection, this set, which typically comprises 15 to 20 pairs of electrodes, did not change during the stimulation campaign.

During the experiments, bioimpedance measurements were performed before and after each stimulation and in some cases after resting periods (see II-E for details).

B. ELECTRONICS FOR STIMULATION

A complete stimulation system (Fig. 3) was designed to combine *in vitro* stimulation and bioimpedance measurement. This system includes a programmable arbitrary waveform generator (*Agilent 33120A*), used as a stimulator triggering physiological contractions. A custom Python software was written to configure stimulation patterns on the programmable waveform generator. These patterns are composed of a series of asymmetric biphasic pulses to ensure charge-balancing and safe stimulation [33]. As illustrated in Fig. 3(b), individual pulses have adjustable amplitude Ip (from 0.5 mA to 55 mA, 0.5 mA step), pulse frequency f (from 0.1 Hz to 100 Hz, 0.1 Hz step), and pulse duration Tp (from 1 ms to 1/3f, 1 ms step). Each positive pulse delivers a charge quantity equal to Ip × Tp. Pause times are also possible.

The system includes a PCB with 6 demultiplexers, to deliver up to 6 stimulation patterns to 6 culture wells. All 6 stimulation voltages and currents are recorded through an integrated oscilloscope (*Analog Discovery 2*, Digilent, sampling rate 100 Msamples/s) and can be monitored on a computer. The *Analog Discovery 2* also handles the synchronization of the demultiplexers and the generator.

Finally, to deliver electrical stimuli to the wells, we designed a PCB that interfaces with the custom support developed for the MEA (Fig. 2). It features two carbon electrodes immersed in the culture medium (4 mm × 4 mm × (h) 22.5 mm), cut from a graphite plate.

C. MUSCLE CELLS CULTURE

Before cell seeding, MEAs were cleaned with ethanol and sterilized in autoclave at 56°C overnight. Then, their surface were coated with Matrigel (5% in *Dulbecco's Modified Eagle's Medium, DMEM*).

C2C12 cells (< 10 passages) were seeded on MEAs at a density of 2000 cells/well. Cells were cultured in 1 mL of growth medium comprising DMEM supplemented with 10% fetal bovine serum and 1% penicillin-streptomycin. Three days after plating cells reached ∼90% confluence. Differentiation into myotubes was then induced by switching the growth medium to a differentiation medium comprising DMEM supplemented with 2% horse serum and 1% penicillin-streptomycin. The differentiation medium was changed every day.

After 5 days of differentiation, the cells were used for experiments. During the experiments, the medium was changed daily, before each stimulation session (see II-E). Cells were maintained in an incubator at 37°C under 5% CO_2 atmosphere.

D. MONITORING AND ANALYSIS OF MYOTUBES CONTRACTION

Our setup allows visual monitoring of the cells out of the incubator. To evaluate the contractile activity of myotubes, we used a camera (*SCOP-CAM4K, ScopPro*) mounted on an inverted microscope. During the stimulation sessions, we recorded ∼10-second videos of each well every hour, at a frame rate of 60 frames per second and at a resolution of 3840 × 2160 (∼8 MPixels).

Image analysis was performed using an ad hoc Python software and the OpenCV library. The program performs a grayscale conversion (256 values; white: 255, black: 0) of video frames, then computes the absolute difference between a reference image (first image, without contraction) and the next frames:

$$\text{img}_{\text{result}} = |\text{img}_{\text{i}} - \text{img}_{\text{ref}}| \quad (1)$$

where img_{i} is the i-th image and img_{ref} the reference image. If there is no motion, pixels of the resulting images ($\text{img}_{\text{result}}$) have a low value, whereas pixels in a region with myotubes contractions have a higher value. Finally, the mean pixel intensity of the resulting image is computed, which quantifies a distance to the reference image: the more movement (and therefore contractions), the higher the mean pixel intensity.

We also visually evaluated the contractile activity, with the following observation criteria:

- Ø: no contractions
- +: < 25% of the MEA surface contracting
- ++: 25-50% of the MEA surface contracting
- +++: 50-75% of the MEA surface contracting
- ++++: > 75% of the MEA surface contracting
- s+: some spontaneous contractions

E. STIMULATION AND MONITORING SCENARIOS

The elementary stimulation pulses were bipolar current pulses as shown in Fig. 3(b), with the following parameters: Ip = 20 mA, Tp = 5 ms, in line with the literature [16], [17], [25], [26], [34].

To study the effect of stimulation frequency and quantity of charge, three stimulation patterns were considered (Fig. 4(a)):

- Pattern 1: continuous 1 Hz (f = 1 Hz)
- Pattern 2: intermittent 10 Hz (f = 10 Hz), 5 pulses at 10 Hz every 5 s
- Pattern 3: intermittent 10 Hz (f = 10 Hz), 10 pulses at 10 Hz every 5 s

Stimulation pattern 1 was intended to check the responsiveness of the cells and to endow contractile activity by triggering twitch contractions [25], [35]. Patterns 2 and 3 were used to trigger tetanic contractions.

Patterns 1 and 2 have the same number of pulses over a period of 5 s (i.e. the same quantity of charge), whereas pattern 3 has twice that number over the same period (i.e. double quantity of charge).

To study the effect of stimulation periods and resting periods, we performed multiple stimulation scenarios (Fig. 4(b)) during 2 experiments using an overall of 6 MEAs (2 series of 3 MEAs). For each experiment, two MEAs (STIM1-2 and STIM3-4 respectively) received actual stimulation while the third one was used for control (CTRL1 and CTR2 respectively) without stimulation.

For the first series, stimulation pattern 1 was applied for 8 hours on day 1 and day 2. Then, STIM1 and STIM2 received stimulation pattern 2 for 2 hours, followed by a 2- (STIM1) or 4-hour (STIM2) rest, and again the same pattern for 2 hours. Finally, on the last day, the same pattern was applied for a longer duration: 4 (STIM2) or 6 (STIM1) hours. For this series, bioimpedance measurements were performed immediately before and after each stimulation period.

For the second series, stimulation pattern 1 was also applied for 8 hours on day 1. The next day, STIM3 and STIM4 received the stimulation pattern 3 for 2 hours, followed by a 2- (STIM3) or 4-hour (STIM4) resting period, then again the same pattern for 2 hours. On the last day, the same pattern was applied for a longer period: 4 (STIM3) or 6 (STIM4) hours. For this series, bioimpedance measurements were made before stimulation, after stimulation, and after the overnight break (before the culture medium change).

III. RESULTS

A. BIOLOGICAL MODEL AND STIMULATION SYSTEM VALIDATION

C2C12 muscle cells were cultured on 6 MEAs and differentiated for 5 days, forming long myotubes (up to several millimeters) about 20 to 50 μm wide (Fig. 5(a)). Without any stimulation, we observed some spontaneous contractions that testify for the successful formation of functional myotubes.

Stimulation scenarios, performed as described in II-E after 5 days of differentiation, effectively trigger contractile activity in myotubes which were camera-monitored. Image analysis shows that myotubes displacement is synchronous to the stimulation patterns, while the movement amplitude can change over time. Fig. 5(b) illustrates the presence and profile of contraction, quantified by the mean pixel intensity (see II-D) for 1 Hz (pattern 1) and 10 Hz (patterns 2 and 3) stimulation. As expected, 1 Hz stimulation triggers twitch contractions (Fig. 5(b), top panel), while 10 Hz stimulation triggers tetanic contractions (Fig. 5(b), middle and bottom panels).

Contractile response to stimulation persists up to 4 days, then cells tend to detach from the MEA substrate and weak contractile activity is observed.

B. DEFINITION OF A BIOIMPEDANCE-BASED METRIC

For all experiments, bioimpedance measurements were performed on MEA electrode pairs before cell seeding (only PBS on MEA) and after the 5-day differentiation phase (at D5). Fig. 6(a) shows the resulting impedance spectrum between 100 Hz and 10 MHz (mean over 10-15 electrodes pairs for each experiment) without cells and after cell differentiation for the 6 MEAs considered in this study.

As expected [29], we observe three phases in the impedance figures before cell seeding (solid lines in Fig. 6(a)): (1) a capacitive interface effect, known as electrode polarization, predominant at low frequencies (100 Hz-10 kHz); (2) a resistive region related to the PBS medium conductivity between 10 kHz and 1 MHz; (3) a parasitic capacitance effect above 1 MHz. Measurements after cell seeding and differentiation (dashed lines in Fig. 6(a)) show that cell presence mostly increases impedance between

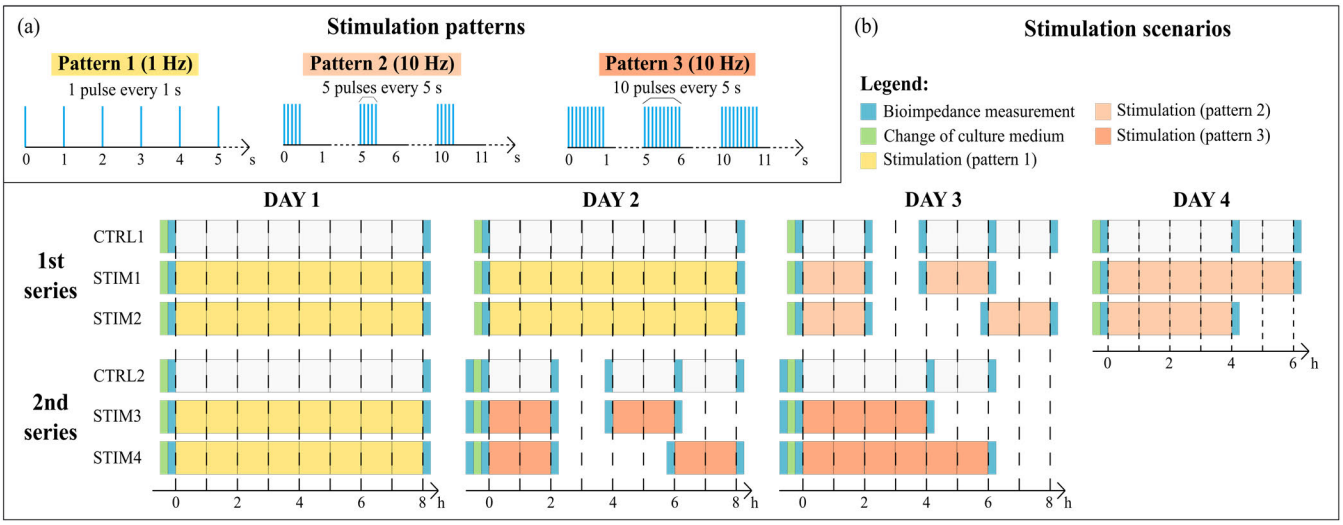

FIGURE 4. (a) Stimulation patterns: pattern 1 (continuous 1 Hz elementary pulses), pattern 2 (intermittent 10 Hz delivering 5 elementary pulses ever 5 s), and pattern 3 (intermittent 10 Hz delivering 10 elementary pulses every 5 s). (b) Stimulation scenarios carried out during the 2 series of experiments (1st series: CTRL1, STIM1, STIM2 during 4 days; 2nd series: CTRL2, STIM3, STIM4 during 3 days). Colors indicate the timing and type of stimulation pattern as well as the timing of bioimpedance measurement and culture medium changes. Resting periods are in white and in-between stimulation scenarios (overnight, approx. 15 hours).

1 kHz and 100 kHz: in this frequency range, cells are essentially non-conductive due to capacitive properties of their membrane. The current flows around the cells and the impedance reflects only the interface and extracellular properties. Beyond 100 kHz, the parasitic effects of the electrode tracks mask the intracellular bioimpedance. Therefore 1 kHz-100 kHz appears as the relevant frequency region of interest to investigate stimulation-induced changes in myotubes.

In that region of interest, the impedance modulus response varies between electrode pairs, typically in the range 50 - 500 kΩ, depending on individual myotubes morphology and orientation. Fig. 6(b) shows the impedance spectrum computed for all measured electrode pairs in a single MEA. To provide an estimate of typical behavior, we considered mean impedance values for each MEA in the following results analysis and discussions. We acknowledge that some variation of mean impedance is observed between MEAs (Fig. 6(a)) due to the intrinsic variability in the myotubes culture process.

Bioimpedance measured at frequencies of about 10 kHz display the greatest range of variation. Based on this observation, the metric chosen to analyze experimental results is the relative variation of the mean bioimpedance module at 10 kHz.

C. EFFECT OF STIMULATION ON CONTRACTILE ACTIVITY

In addition to bioimpedance variations, we also monitored how stimulation and resting scenarios affected the contractile activity. During each stimulation session, contractile activity increased over time, as evidenced by increased motion amplitudes and contraction speeds. Fig. 7 illustrates this phenomenon. Stimulation pattern 1 (1 Hz) elicited a fast increase in twitch contraction amplitude and speed, noticeable in less than 2 hours (Fig. 7(a)). Stimulation patterns 2 and 3 (10 Hz) at first induced fused tetanic contractions. After 2 hours, unfused tetanic contractions (series of contractions with partial relaxation) were observed (Fig. 7(b) and 7(c)). Movement amplitude was found to be smaller as stimulation resumed after resting periods, but ultimately increased over time resulting in unfused tetanic contractions after a couple of hours. This post-resting amplitude decrease is more noticeable after longer breaks, especially after overnight breaks.

D. BIOIMPEDANCE RESPONSE

1) EFFECT OF 1 Hz STIMULATION

On day 1, bioimpedance measurements were performed on STIM1-2 and STIM3-4 before and after an 8-hour application of stimulation pattern 1 (1 Hz). The mean bioimpedance values at 10 kHz before and after stimulation are presented in Fig. 8(a) for CTRL1, STIM1-2 and in Fig. 8(b) for CTRL2, STIM3-4. Initial values are between 94 kΩ and 293 kΩ. Numerical bioimpedance values and relative variations are reported in Table 1.

For both series of 3 MEAs, we observed a decrease in the bioimpedance on all MEAs after 8 hours, with or without stimulation. However, the impedance decline is much larger (almost twice) in the 2 stimulated MEAs than in the control MEA.

Bioimpedance of CTRL2, STIM3-4 was also measured after an overnight resting period. Fig. 8(b) shows that the impedance decrease is lower during this resting period than during the stimulation phase.

On day 2, after an overnight break and a change of the culture medium, we measured the bioimpedance of CTRL1 and STIM1-2 and again we applied the 1 Hz stimulation pattern

TABLE 1. Relative variation of the mean bioimpedance module at 10 kHz and contractile activity level during the 1 Hz stimulation scenarios (pattern 1).

	DAY :	DAY 1						DAY 2		
	MEA :	CTRL1	STIM1	STIM2	CTRL2	STIM3	STIM4	CTRL1	STIM1	STIM2
Stimulation parameters	Pattern	/			/			/		
	Duration (h)	8	8	8	8	8	8	8	8	8
	Pause time before stimulation (h)	/	/	/	/	/	/	>12h		
Bioimpedance variations	Relative variations (%)	-18.92	-33.79	-32.61	-13.47	-23.76	-20.97	-22.91	-18.56	-23.02
	Relative variations per hour (%)	-2.37	-4.22	-4.08	-1.68	-2.97	-2.62	-2.86	-2.32	-2.88
Contractile activity		s+	+++	+++	s+	++++	++++	s+	+	+++

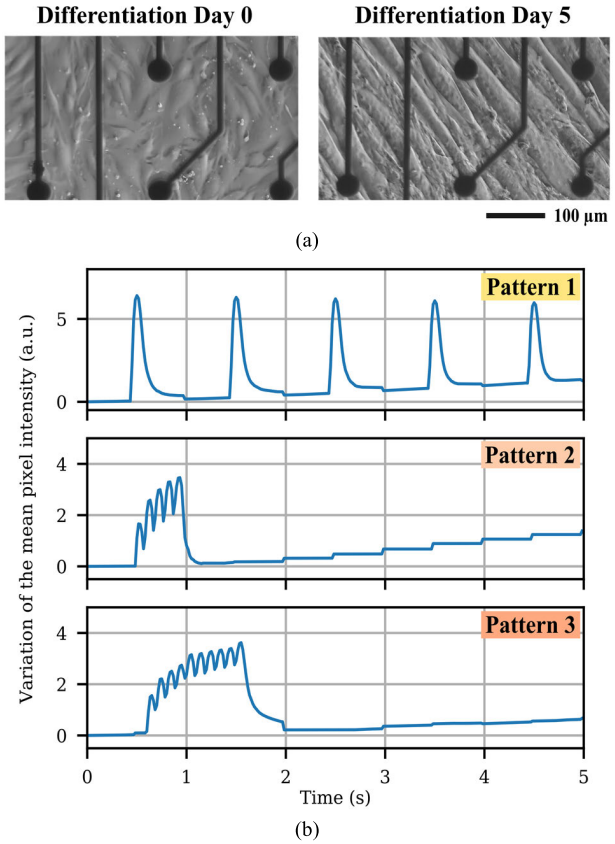

FIGURE 5. (a) Myotubes formation in C2C12 cells cultured on MEA: (left) before differentiation, C2C12 myoblasts, (right) after 5 days of differentiation (D5), C2C12 myotubes (bar: 100 μm). (b) Image analysis of contractile activity induced by electrical stimulation using: (top) pattern 1 on STIM4, day 1, (middle) pattern 2 on STIM2, day 3, (bottom) pattern 3 on STIM3, day 2.

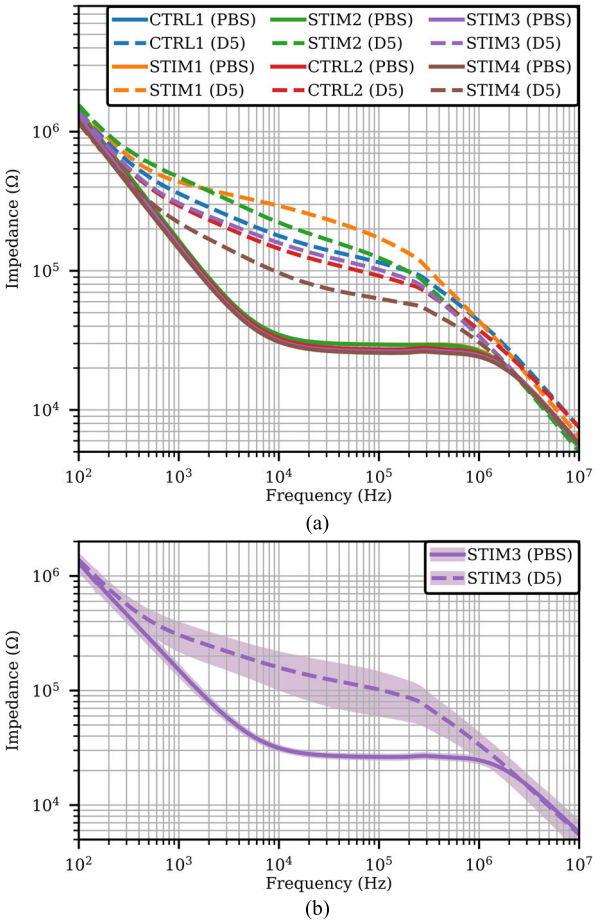

FIGURE 6. (a) Impedance spectroscopy before cell seeding with PBS (solid line) and after 5 days of differentiation (dashed line) on the 6 MEAs, mean values for 10-15 electrodes pairs. (b) One MEA (STIM3), all 15 measured electrodes, mean value ± standard deviation. PBS = only PBS on the MEA; D5 = myotubes on MEA at 5th day of differentiation.

on STIM1-2 for 8 hours. We observed a decreased contractile activity on the two stimulated MEAs after the overnight break, as mentioned in III-C. Fig. 8(c) and Table 1 show that the bioimpedance decrease was still significant with a similar rate for all MEAs, stimulated or not.

2) EFFECT OF 10 Hz STIMULATION – PATTERN 2

All day 3 metrics are presented in Table 2. Bioimpedance was measured on CTRL1, STIM1 and STIM2, and the last two were electrically stimulated for 2 hours with pattern 2 (10 Hz). As shown in Fig. 9(a) and Fig. 9(b), initial values were between 140 kΩ and 273 kΩ.

Similarly to day 2, we observed a low contractile activity on the stimulated MEAs, which presented a relative bioimpedance variation similar or lower than the control MEA.

Stimulation pattern 2 was applied again for 2 hours to STIM1 and STIM2, after a 2-hour break and 4-hour break,

TABLE 2. Relative variation of the mean bioimpedance module at 10 kHz and contractile activity level during the 10 Hz stimulation scenarios (pattern 2).

	DAY :	DAY 3							DAY 4			
	MEA :	CTRL1			STIM1		STIM2		CTRL1		STIM1	STIM2
Stimulation parameters	Pattern	/			Pattern 2				/		Pattern 2	
	Duration (h)	2	2	2	2	2	2	2	4	6	6	4
	Pause time before stimulation (h)	>12h	2	4	>12h	2	>12h	4	>12h			
Bioimpedance variations	Relative variations (%)	-8.07	-6.26	-3.67	-2.95	-18.90	-9.57	-9.32	-4.37	-12.68	-29.38	-31.17
	Relative variations per hour (%)	-4.04	-3.13	-1.84	-1.48	-9.45	-4.79	-4.66	-1.09	-2.11	-4.90	-7.79
Contractile activity		s+	s+	Ø	+	+	++	++	Ø	Ø	+	+

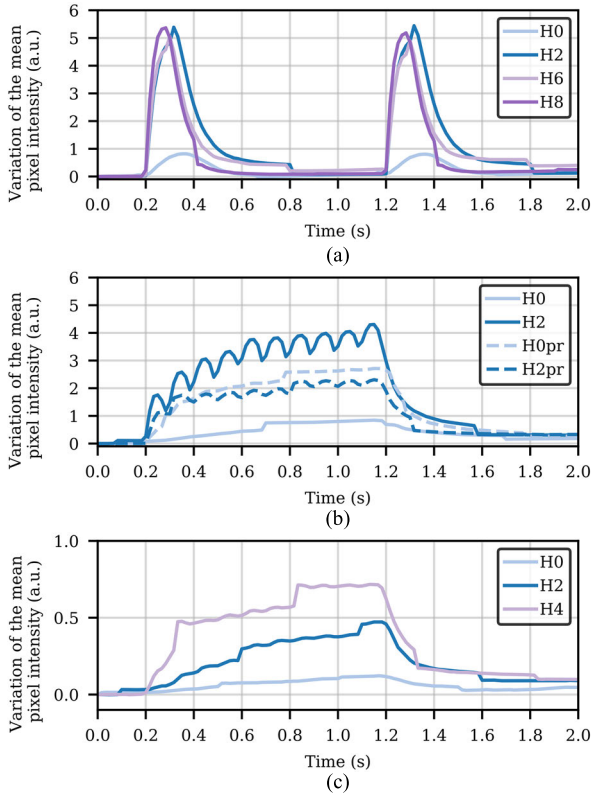

FIGURE 7. Plots of mean pixel intensity variation (relative to the initial value at time 0). (a) Twitch contractions in response to 1 Hz stimulation (pattern 1). Measurements at stimulation start (H0) then after 2, 6 and 8 hours (H2, H6, H8) on STIM3 at day 1. (b) Tetanic contractions in response to 10 Hz stimulation (pattern 3). Measurement on STIM3 at day 2, every 2 hours. H0: start of the first stimulation period; H2: end of the first 2-hour stimulation period; H0pr: start of the second stimulation period after 2-hour rest; H2pr: end of the second 2-hour stimulation period. (c) Tetanic contractions in response to 10 Hz stimulation (pattern 3). Measurements at stimulation start (H0) then every 2 hours (H2, H4) on STIM3 at day 3.

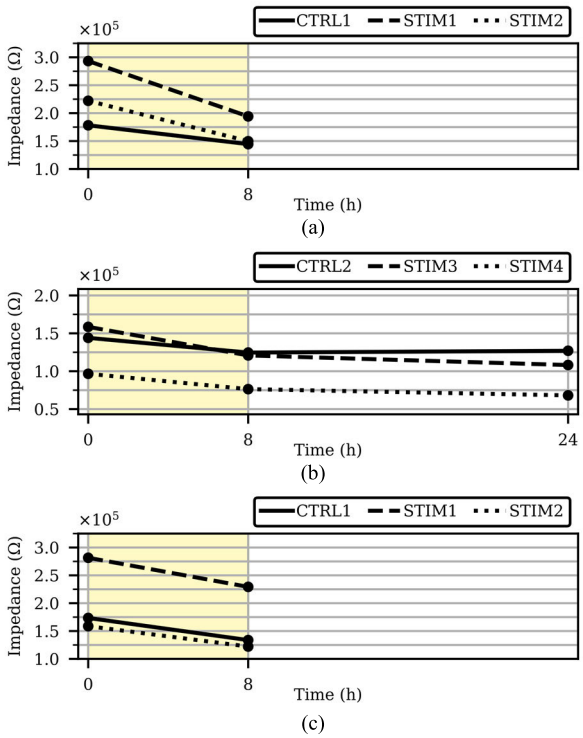

FIGURE 8. Mean bioimpedance at 10 kHz over time during day 1 for CTRL1, STIM1-2 (a), and for CTRL2, STIM3-4 (b), and during day 2 for CTRL1, STIM1-2 (c). The yellow areas indicate the stimulation periods (pattern 1).

respectively. Again, all MEAs presented a decrease in the relative bioimpedance values (Table 2, Fig. 9(a) and 9(b)). Interestingly enough, STIM1 presented a decrease rate twice bigger than STIM2, in accordance with its shorter resting period; both stimulated MEAs presented a higher bioimpedance decrease than CTRL1.

Finally, on day 4, after an overnight resting time, we investigated the effect of stimulation pattern 2 over a longer period. After 4 hours and 6 hours respectively, both STIM1 and STIM2 exhibited similar bioimpedance decrease rates, much larger than CTRL1 (Table 2, Fig. 9(c) and 9(d)). We also noted that the variations during 4 hours or 6 hours of stimulation were greater than those measured after only 2 hours of stimulation with the same pattern (Table 2).

3) EFFECT OF 10 Hz STIMULATION – PATTERN 3

On day 2, we measured the bioimpedance on CTRL2, STIM3 and STIM4, and applied stimulation pattern 3 (10 Hz) for 2 hours to STIM3-4. Before stimulation, CTRL2, STIM3 and STIM4 showed bioimpedances of 173 kΩ, 176 kΩ and 93 kΩ,

TABLE 3. Relative variation of the mean bioimpedance module at 10 kHz and contractile activity level during the 10 Hz stimulation scenarios (pattern 3).

	DAY :	DAY 2							DAY 3			
	MEA :	CTRL2			STIM3		STIM4		CTRL2		STIM3	STIM4
Stimulation parameters	Pattern	/			Pattern 3				/		Pattern 3	
	Duration (h)	2	2	2	2	2	2	2	4	6	4	6
	Pause time before stimulation (h)	>12h	2	4	>12h	2	>12h	4	>12h			
Bioimpedance variations	Relative variations (%)	-3.81	0.95	-6.49	-21.68	-8.86	-16.06	-6.89	-17.78	-25.33	-24.40	-21.36
	Relative variations per hour (%)	-1.91	0.48	-3.25	-10.84	-4.43	-8.03	-3.45	-4.45	-4.22	-6.10	-3.56
Contractile activity		Ø	Ø	Ø	+++	++	++	+	Ø	Ø	+	+

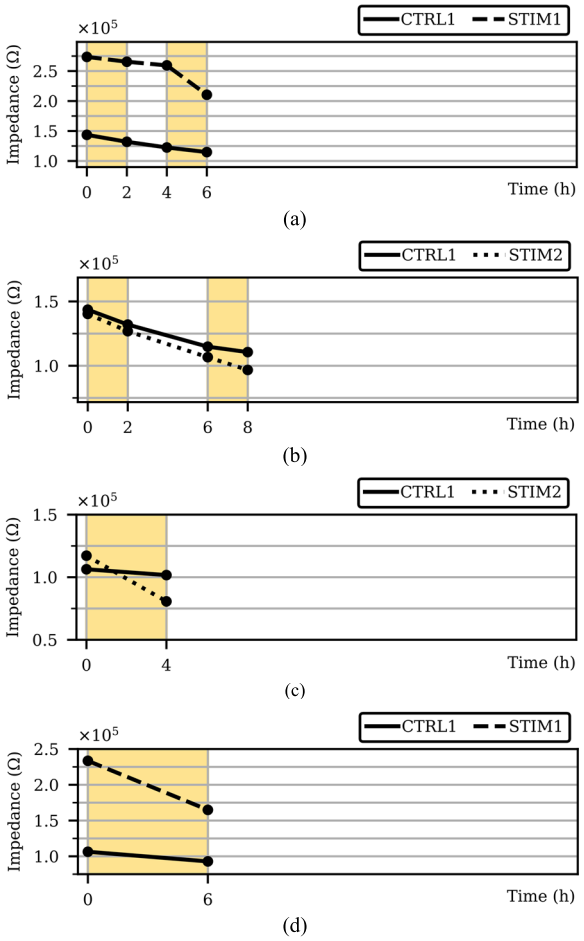

FIGURE 9. Mean bioimpedance at 10 kHz over time during day 3 for CTRL1 and STIM1 (a), CTRL1 and STIM2 (b), and during day 4 for CTRL1 and STIM2 (c), CTRL1 and STIM1 (d). The light orange areas indicate the stimulation periods (pattern 2).

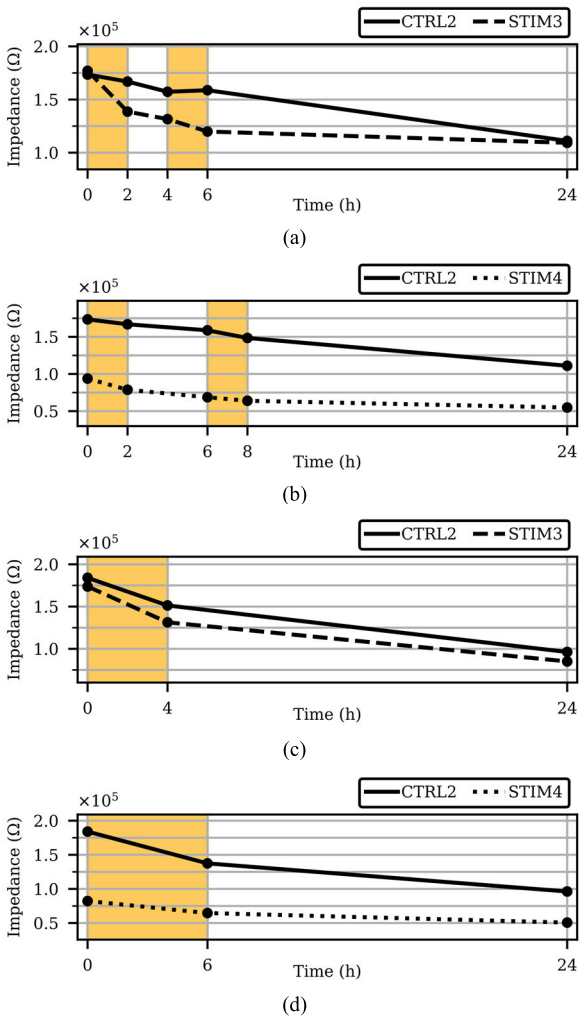

FIGURE 10. Mean bioimpedance at 10 kHz over time during day 2 for CTRL2 and STIM3 (a), CTRL2 and STIM4 (b), and during day 2 for CTRL2 and STIM3 (c), CTRL2 and STIM4 (d). The orange areas indicate the stimulation periods (pattern 3).

respectively (Fig. 10(a) and Fig. 10(b)). Again (Table 3), we noticed a greater bioimpedance variation in the two stimulated MEAs than in the control MEA.

After a 2-hour rest for STIM3 and a 4-hour rest for STIM4, stimulation pattern 3 was applied again for 2 hours. STIM3 bioimpedance decreased significantly faster than CTRL2 while STIM4 bioimpedance decrease rate was similar to CTRL2 (see Table 3, Fig. 9(a) and 9(b)).

Finally, we investigated the effect of pattern 3 on bioimpedance over longer stimulation periods. Before stimulation, CTRL2, STIM3 and STIM4 showed bioimpedances of 184 kΩ, 173 kΩ and 82 kΩ, respectively (Fig. 10(c) and

Fig. 10(d)). STIM3 was then subjected to 4 hours of stimulation while STIM4 was subjected to 6 hours. All bioimpedance values had similar variation ranges, with a slightly greater variation for STIM3 that we relate to its natively higher contractile activity. As observed for pattern 2 in III-D2, the relative variations during 4 or 6 hours of stimulation were larger than those measured after only 2 hours of stimulation with the same pattern (Table 3).

4) STIMULATION PARAMETERS IMPACT

The three stimulation patterns vary by two parameters: the pulse frequency and the number of pulses, over the main 5 s period. We analyzed the bioimpedance relative variation per hour related to these two parameters.

To study the effect of the stimulation pulse frequency, results were compared between the application of patterns 1 and 2, that present the same number of pulses per 5 s period but different frequencies (1 Hz and 10 Hz, respectively). In both series of experiments, we observed that the 10 Hz stimulation (Table 2) was almost systematically associated with a larger bioimpedance decrease rate than the 1 Hz stimulation (Table 1). Thus, the pulse frequency seems to impact the bioimpedance.

Similarly, we compared the effect of the number of pulses with patterns 2 and 3, that had the same frequency (10 Hz) but a different number of pulses (5 and 10, respectively) over the same 5-second period. Comparing results for pattern 2 on STIM1 and STIM2 (Table 2) with results for pattern 3 for STIM3 and STIM4 (Table 3), we observed no significant difference in the range of bioimpedance relative variations (between -1.5% and -11%). We conclude that the number of pulses has less impact than the frequency on the bioimpedance variations.

Finally, we studied the combined effect of the 2 stimulation parameters by comparing experiment results obtained with patterns 1 and 3 on STIM3 and STIM4. In Tables 1 and 3, we observe a systematically and significantly larger bioimpedance decrease rate per hour for pattern 3 (below 3% for pattern 1, up to 10% for pattern 3). Modifying both the pulses frequency and the injected charge quantity seems to be the best way to impact the myotubes impedance.

IV. DISCUSSION

We present an *in vitro* setup that allows not only bioimpedance and visual monitoring of muscle cells, but also contraction-inducing electrical stimulation.

We successfully cultured and differentiated muscle cells on MEAs, resulting in functional myotubes after 5 days of differentiation. Very few studies have performed muscle cell cultures on MEAs: most ([18], [30], [31]) use primary cells, while only two studies involve the C2C12 cell line [36], [37]. This cell line is mostly cultured in conventional culture wells and stimulated with commercial carbon electrodes [16], [17], [25], [26]. To our knowledge, our setup is the first to combine a configurable electrical stimulation system with macroelectrodes and an impedance measurement system using MEAs. Only [30] succeeded in electrically stimulating myotubes, using selective MEA electrodes, whereas our setup allows stimulation of the whole culture. We have demonstrated that our stimulation system can induce myotubes contractions synchronous to the stimulation frequency. As expected [38], 1 Hz stimulation elicited twitch contractions, while a 10 Hz stimulation frequency resulted in fused or unfused tetani. The contractile activity was found to be progressively enhanced (increase of amplitude and speed contraction) during every single stimulation session, consistent with observations from [25] and [39].

Although electrically induced contractions were present during the 4 days of experiments, we observed a decrease trend in contractile activity over the days, after each overnight break. The cells showed vigorous contractions the first day, whereas after an overnight rest, the contractions were weaker and rarer. This may be due to the long overnight break times ($>$ 12h) without stimulation [16]: applied low frequency (0.1 Hz) stimulation during pause time to prevent the decrease in contractile activity. Termination of electrical stimulation appears to induce an atrophy-like response and a decay of the sarcomere structure [39]. After $\sim$10 days of culture (including the 5 days of differentiation), the cells start to detach from the MEA surface, even when it is coated with extracellular matrix proteins (Matrigel) [3]. This phenomenon does not seem to be related to the stimulation as it was also observed with control MEAs.

We previously published a bioimpedance measurement system in [29], that uses an MEA model with SiN substrate passivation and PEDOT-covered electrodes that present visible degradation after a few experiments. In this study, we used a new MEA model with SU8 passivation and Pt-Black electrodes where electrode quality was stable over time (verified with impedance characterization, data not shown). Furthermore, we observed that cell adhesion was better on the new model, which we attribute to the different passivation layer. Nevertheless, the cell-free impedance characterization with PBS gave similar and reproducible results for the two MEAs models. We demonstrate that myotubes on the MEA can be detected by an increase of the mean bioimpedance module between 1 kHz and 100 kHz, although this increase varies between experiments. Past studies [24], [40] explain these variations of bioimpedance by differences in cell morphology and orientation. This issue could be limited by controlling the orientation of the myotubes during differentiation either mechanically with PDMS trenches [41], or with an adequate coating pattern as in [36], [42]. Moreover, myotubes oriented parallel to the electrical field would result in enhanced cell excitation (lower currents required), as reported by [38].

We evaluated the impact of 3 stimulation patterns: 1 Hz continuous, 10 Hz discontinuous with a series of 5 pulses or 10 pulses over a period of 5 seconds. The impedance of control MEAs decreased over time even without stimulation. However, stimulated MEAs presented larger impedance variations, further pronounced with longer stimulation.

In these same MEAs, bioimpedance variation was lower during resting times than during stimulation periods. Interestingly, bioimpedance decrease during stimulation was even lower after longer rests.

We also observed that increasing stimulation frequency, while keeping the same injected charge quantity, led to a greater bioimpedance decline. Conversely, doubling the number of pulses without increasing the stimulation frequency had limited impact on the bioimpedance variations. Lastly, the joint increase of stimulation frequency and number of pulses (thus the charge quantity) caused greater bioimpedance decrease. Thanks to the system's capacity to deliver up to 100 Hz stimulation pulses, the effect of higher stimulation frequency will be investigated in future experiments.

Experiments showed that the parameters of the stimulation patterns do affect the bioimpedance differently, yet these results are to be considered with a clear understanding of the limitations of our setup: it is not automated, resulting in time-consuming measurements, and does not allow measurements in the incubator. Measurements are therefore influenced by temperature variations during the measurement phase.

In this paper, we only analyzed the relative variation of bioimpedance module at 10 kHz. For a more comprehensive study, the whole bioimpedance spectrum could be fitted with mathematical models (e.g. Cole-Cole [43] or Fricke model [44]) to relate model parameter changes to electrical stimulation scenarios and derive a fatigue metric. Analyzing the phase could also reveal additional information about the myotubes physiological state.

Finally, video analysis to assess contractile activity has proved to be challenging as extracting a metric to quantify that activity requires eliminating interfering movements. [45] cites some of these motions: camera noise, changes in brightness, setup vibrations, and floating cellular debris. Video compression also generates a loss of pixel information [46] and keyframes artifacts [45] that have to be handled. These issues limited the use of video analysis in this paper to coarse examination of contraction types on short periods (few seconds).

A more resolutive alternative to explore contractile activity at the cellular level consists in recording electrical activity - typically spiking - through the already present MEA electrodes, which is planned in future experiments.

Even though we demonstrated quantitative bioimpedance variations and qualitative changes in contractile response, more experiments and analyses (e.g. biochemical parameters) are necessary to establish a formal link between them, or with global phenomena like muscle fatigue.

V. CONCLUSION

In this work, we present a new tool to monitor *in vitro* muscle physiology and behavior during electrical stimulation. This novel system allows to culture muscle cells on an MEA and to differentiate them into functional and contractile myotubes. Stimulation patterns are fully configurable and successfully trigger myotubes' contractions. The physiological state of myotubes is monitored non-invasively by bioimpedance spectroscopy and video recording. Proof of concept experiments validate the system and demonstrate that bioimpedance varies with stimulation and rest, which may reflect myotubes' metabolic and physiological changes. Stimulated cells showed a greater decrease in bioimpedance than unstimulated ones. In addition, bioimpedance variations during stimulation appeared smaller after longer breaks. We also found that increasing stimulation frequency or duration resulted in greater bioimpedance decline. To our knowledge, our system is the first *in vitro* setup allowing the direct monitoring of muscle cell bioimpedance in response to electrical stimulation.

ACKNOWLEDGMENT

The authors thank Dr. Gilles Carnac (PhyMedExp, UMR UM—CNRS 9214—Inserm U1046, and Montpellier) for providing cell lines and Prof. Noëlle Lewis, Dr. Julien Claudel, and Dr. Florian Kölbl for fruitful discussions and guidance.

REFERENCES

[1] S. Carter and T. P. J. Solomon, "In vitro experimental models for examining the skeletal muscle cell biology of exercise: The possibilities, challenges and future developments," *Pflügers Archiv, Eur. J. Physiol.*, vol. 471, no. 3, pp. 413–429, Mar. 2019, doi: 10.1007/s00424-018-2210-4.

[2] N. Nikolić, S. W. Görgens, G. H. Thoresen, V. Aas, J. Eckel, and K. Eckardt, "Electrical pulse stimulation of cultured skeletal muscle cells as a model for in vitro exercise–possibilities and limitations," *Acta Physiol.*, vol. 220, no. 3, pp. 310–331, Jul. 2017, doi: 10.1111/apha.12830.

[3] A. Khodabukus, N. Prabhu, J. Wang, and N. Bursac, "In vitro tissue-engineered skeletal muscle models for studying muscle physiology and disease," *Adv. Healthcare Mater.*, vol. 7, no. 15, Aug. 2018, Art. no. 1701498, doi: 10.1002/adhm.201701498.

[4] D. G. Allen, G. D. Lamb, and H. Westerblad, "Skeletal muscle fatigue: Cellular mechanisms," *Physiol. Rev.*, vol. 88, no. 1, pp. 287–332, Jan. 2008, doi: 10.1152/physrev.00015.2007.

[5] J. Mizrahi, "Fatigue in muscles activated by functional electrical stimulation," *Crit. Rev. Phys. Rehabil. Med.*, vol. 9, no. 2, pp. 93–129, 1997.

[6] N. K. Vøllestad, "Measurement of human muscle fatigue," *J. Neurosci. Methods*, vol. 74, no. 2, pp. 219–227, Jun. 1997, doi: 10.1016/S0165-0270(97)02251-6.

[7] J. Finsterer, "Biomarkers of peripheral muscle fatigue during exercise," *BMC Musculoskeletal Disorders*, vol. 13, no. 1, p. 218, Nov. 2012, doi: 10.1186/1471-2474-13-218.

[8] T. Takaishi, T. Ono, and Y. Yasuda, "Relationship between muscle fatigue and oxygen uptake during cycle ergometer exercise with different ramp slope increments," *Eur. J. Appl. Physiol. Occupational Physiol.*, vol. 65, no. 4, pp. 335–339, 1992, doi: 10.1007/BF00868137.

[9] W. Laube, J. Martin, J. Tank, R. M. Baevski, and E. Schubert, "Heart rate variability—An indicator of the muscle fatigue after physical exercise," *Perfusion*, vol. 9, no. 5, pp. 225–229, 1996.

[10] M. Cifrek, V. Medved, S. Tonković, and S. Ostojić, "Surface EMG based muscle fatigue evaluation in biomechanics," *Clin. Biomech.*, vol. 24, no. 4, pp. 327–340, May 2009, doi: 10.1016/j.clinbiomech.2009.01.010.

[11] L. Li, H. Shin, X. Li, S. Li, and P. Zhou, "Localized electrical impedance myography of the biceps brachii muscle during different levels of isometric contraction and fatigue," *Sensors*, vol. 16, no. 4, p. 581, Apr. 2016, doi: 10.3390/s16040581.

[12] B. Fu and T. J. Freeborn, "Biceps tissue bioimpedance changes from isotonic exercise-induced fatigue at different intensities," *Biomed. Phys. Eng. Exp.*, vol. 4, no. 2, Feb. 2018, Art. no. 025037, doi: 10.1088/2057-1976/aaabed.

[13] T. J. Freeborn and B. Fu, "Time-course bicep tissue bio-impedance changes throughout a fatiguing exercise protocol," *Med. Eng. Phys.*, vol. 69, pp. 109–115, Jul. 2019, doi: 10.1016/j.medengphy.2019.04.006.

[14] L. K. Huang, L. N. Huang, Y. M. Gao, Ž. L. Vasić, M. Cifrek, and M. Du, "Electrical impedance myography applied to monitoring of muscle fatigue during dynamic contractions," *IEEE Access*, vol. 8, pp. 13056–13065, 2020, doi: 10.1109/ACCESS.2020.2965982.
[15] C. W. McAleer, A. S. T. Smith, S. Najjar, K. Pirozzi, C. J. Long, and J. J. Hickman, "Mechanistic investigation of adult myotube response to exercise and drug treatment in vitro using a multiplexed functional assay system," *J. Appl. Physiol.*, vol. 117, no. 11, pp. 1398–1405, Dec. 2014, doi: 10.1152/japplphysiol.00612.2014.
[16] T. Nedachi, H. Fujita, and M. Kanzaki, "Contractile C_2C_{12} myotube model for studying exercise-inducible responses in skeletal muscle," *Amer. J. Physiol.-Endocrinol. Metabolism*, vol. 295, no. 5, pp. E1191–E1204, Nov. 2008, doi: 10.1152/ajpendo.90280.2008.
[17] Y. Manabe, S. Miyatake, M. Takagi, M. Nakamura, A. Okeda, T. Nakano, M. F. Hirshman, L. J. Goodyear, and N. L. Fujii, "Characterization of an acute muscle contraction model using cultured C_2C_{12} myotubes," *PLoS ONE*, vol. 7, no. 12, Dec. 2012, Art. no. e52592, doi: 10.1371/journal.pone.0052592.
[18] M. K. Lewandowska, E. Bogatikov, A. R. Hierlemann, and A. R. Punga, "Long-term high-density extracellular recordings enable studies of muscle cell physiology," *Frontiers Physiol.*, vol. 9, p. 1424, Oct. 2018. [Online]. Available: https://www.frontiersin.org/articles/10.3389/fphys.2018.01424
[19] S. Grimnes and Ø. G. Martinsen, *Bioimpedance and Bioelectricity Basics*, 2nd ed. London, U.K.: Academic, 2008.
[20] I. Giaever and C. R. Keese, "Use of electric fields to monitor the dynamical aspect of cell behavior in tissue culture," *IEEE Trans. Biomed. Eng.*, vol. BME-33, no. 2, pp. 242–247, Feb. 1986, doi: 10.1109/TBME.1986.325896.
[21] G. H. Lee, J.-C. Pyun, and S. Cho, "Electrical impedance characterization of cell growth on interdigitated microelectrode array," *J. Nanosc. Nanotechnol.*, vol. 14, no. 11, pp. 8342–8346, Nov. 2014, doi: 10.1166/jnn.2014.9929.
[22] S. M. Murphy, M. Kiely, P. M. Jakeman, P. A. Kiely, and B. P. Carson, "Optimization of an in vitro bioassay to monitor growth and formation of myotubes in real time," *Biosci. Rep.*, vol. 36, no. 3, May 2016, Art. no. e00330, doi: 10.1042/BSR20160036.
[23] I. Park, Y. Hong, Y.-H. Jun, G.-Y. Lee, H.-S. Jun, J.-C. Pyun, J.-W. Choi, and S. Cho, "Electrical impedance monitoring of C_2C_{12} myoblast differentiation on an indium tin oxide electrode," *Sensors*, vol. 16, no. 12, p. 2068, Dec. 2016, doi: 10.3390/s16122068.
[24] S. Rakhilin, G. Turner, M. Katz, R. Warden, J. Irelan, Y. A. Abassi, and D. J. Glass, "Electrical impedance as a novel biomarker of myotube atrophy and hypertrophy," *SLAS Discovery*, vol. 16, no. 6, pp. 565–574, Jul. 2011, doi: 10.1177/1087057111401392.
[25] H. Fujita, T. Nedachi, and M. Kanzaki, "Accelerated de novo sarcomere assembly by electric pulse stimulation in C_2C_{12} myotubes," *Exp. Cell Res.*, vol. 313, no. 9, pp. 1853–1865, May 2007, doi: 10.1016/j.yexcr.2007.03.002.
[26] Z. Orfanos, M. P. O. Gödderz, E. Soroka, T. Gödderz, A. Rumyantseva, P. F. M. van der Ven, T. J. Hawke, and D. O. Fürst, "Breaking sarcomeres by in vitro exercise," *Sci. Rep.*, vol. 6, no. 1, p. 19614, Jan. 2016, doi: 10.1038/srep19614.
[27] Y. Tamura, K. Kouzaki, T. Kotani, and K. Nakazato, "Electrically stimulated contractile activity-induced transcriptomic responses and metabolic remodeling in C_2C_{12} myotubes: Twitch vs. tetanic contractions," *Amer. J. Physiol.-Cell Physiol.*, vol. 319, no. 6, pp. C1029–C1044, Dec. 2020, doi: 10.1152/ajpcell.00494.2019.
[28] A. Khodabukus, L. Madden, N. K. Prabhu, T. R. Koves, C. P. Jackman, D. M. Muoio, and N. Bursac, "Electrical stimulation increases hypertrophy and metabolic flux in tissue-engineered human skeletal muscle," *Biomaterials*, vol. 198, pp. 259–269, Apr. 2019, doi: 10.1016/j.biomaterials.2018.08.058.
[29] A. Bailleul, J. Claudel, F. P. De Gannes, G. N'Kaoua, F. Kolbl, F. Soulier, N. Lewis, S. Bernard, and S. Renaud, "In vitro impedance spectroscopy: A MEA-based measurement bench for myoblasts cultures monitoring," in *Proc. XXXVI Conf. Design Circuits Integr. Syst. (DCIS)*, Nov. 2021, pp. 1–6, doi: 10.1109/DCIS53048.2021.9666172.
[30] C. G. Langhammer, M. K. Kutzing, V. Luo, J. D. Zahn, and B. L. Firestein, "Skeletal myotube integration with planar microelectrode arrays in vitro for spatially selective recording and stimulation: A comparison of neuronal and myotube extracellular action potentials," *Biotechnol. Prog.*, vol. 27, no. 3, pp. 891–895, May 2011, doi: 10.1002/btpr.609.
[31] N. Rabieh, S. M. Ojovan, N. Shmoel, H. Erez, E. Maydan, and M. E. Spira, "On-chip, multisite extracellular and intracellular recordings from primary cultured skeletal myotubes," *Sci. Rep.*, vol. 6, no. 1, p. 36498, Nov. 2016, doi: 10.1038/srep36498.
[32] M. E. Spira and A. Hai, "Multi-electrode array technologies for neuroscience and cardiology," *Nature Nanotechnol.*, vol. 8, no. 2, pp. 83–94, Feb. 2013, doi: 10.1038/nnano.2012.265.
[33] D. R. Merrill, M. Bikson, and J. G. R. Jefferys, "Electrical stimulation of excitable tissue: Design of efficacious and safe protocols," *J. Neurosci. Methods*, vol. 141, no. 2, pp. 171–198, Feb. 2005, doi: 10.1016/j.jneumeth.2004.10.020.
[34] K. Nagamine, H. Sato, H. Kai, H. Kaji, M. Kanzaki, and M. Nishizawa, "Contractile skeletal muscle cells cultured with a conducting soft wire for effective, selective stimulation," *Sci. Rep.*, vol. 8, no. 1, p. 2253, Feb. 2018, doi: 10.1038/s41598-018-20729-y.
[35] K. Nagamine, T. Kawashima, T. Ishibashi, H. Kaji, M. Kanzaki, and M. Nishizawa, "Micropatterning contractile C_2C_{12} myotubes embedded in a fibrin gel," *Biotechnol. Bioeng.*, vol. 105, no. 6, pp. 1161–1167, Apr. 2010, doi: 10.1002/bit.22636.
[36] P. Molnar, W. Wang, A. Natarajan, J. W. Rumsey, and J. J. Hickman, "Photolithographic patterning of C_2C_{12} myotubes using vitronectin as growth substrate in serum-free medium," *Biotechnol. Prog.*, vol. 23, no. 1, pp. 265–268, Feb. 2007, doi: 10.1021/bp060302q.
[37] M. Gabi, T. Sannomiya, A. Larmagnac, M. Puttaswamy, and J. Vörös, "Influence of applied currents on the viability of cells close to microelectrodes," *Integr. Biol.*, vol. 1, no. 1, pp. 108–115, 2009, doi: 10.1039/b814237h.
[38] K.-I. Yamasaki, H. Hayashi, K. Nishiyama, H. Kobayashi, S. Uto, H. Kondo, S. Hashimoto, and T. Fujisato, "Control of myotube contraction using electrical pulse stimulation for bio-actuator," *J. Artif. Organs*, vol. 12, no. 2, pp. 131–137, Jun. 2009, doi: 10.1007/s10047-009-0457-4.
[39] H. Fujita, M. Hirano, K. Shimizu, and E. Nagamori, "Rapid decrease in active tension generated by C_2C_{12} myotubes after termination of artificial exercise," *J. Muscle Res. Cell Motility*, vol. 31, no. 4, pp. 279–288, Dec. 2010, doi: 10.1007/s10974-010-9230-9.
[40] R. Aaron, M. Huang, and C. A. Shiffman, "Anisotropy of human muscle via non-invasive impedance measurements," *Phys. Med. Biol.*, vol. 42, no. 7, pp. 1245–1262, Jul. 1997, doi: 10.1088/0031-9155/42/7/002.
[41] C. G. Langhammer, M. K. Kutzing, V. Luo, J. D. Zahn, and B. L. Firestein, "A topographically modified substrate-embedded MEA for directed myotube formation at electrode contact sites," *Ann. Biomed. Eng.*, vol. 41, no. 2, pp. 408–420, Feb. 2013, doi: 10.1007/s10439-012-0647-8.
[42] P. Bajaj, B. Reddy, Jr., L. Millet, C. Wei, P. Zorlutuna, G. Bao, and R. Bashir, "Patterning the differentiation of C_2C_{12} skeletal myoblasts," *Integrative Biol.*, vol. 3, no. 9, pp. 897–909, Sep. 2011, doi: 10.1039/c1ib00058f.
[43] T. Freeborn and B. Fu, "Fatigue-induced Cole electrical impedance model changes of biceps tissue bioimpedance," *Fractal Fractional*, vol. 2, no. 4, p. 27, Oct. 2018, doi: 10.3390/fractalfract2040027.
[44] N. Herencsar, "An empirical study of fatigue-induced electrical impedance models of biceps tissues," in *Proc. 12th Int. Congr. Ultra Modern Telecommun. Control Syst. Workshops (ICUMT)*, Oct. 2020, pp. 58–61, doi: 10.1109/ICUMT51630.2020.9222426.
[45] T. Grune, C. Ott, S. Häseli, A. Höhn, and T. Jung, "The 'MYOCYTER'—Convert cellular and cardiac contractions into numbers with ImageJ," *Sci. Rep.*, vol. 9, no. 1, p. 15112, Oct. 2019, doi: 10.1038/s41598-019-51676-x.
[46] L. Sala et al., "MUSCLEMOTION: A versatile open software tool to quantify cardiomyocyte and cardiac muscle contraction in vitro and in vivo," *Circulat. Res.*, vol. 122, no. 3, pp. e5–e16, Feb. 2018, doi: 10.1161/CIRCRESAHA.117.312067.

ALEXIA BAILLEUL received the Engineer Diploma and M.Sc. degrees in electronics engineering from CentraleSupélec, Paris, France, in 2019. She is currently pursuing the Ph.D. degree in electrical engineering with the University of Bordeaux, France, with an emphasis in electrical stimulation and bioimpedance.

FLORENCE POULLETIER DE GANNES received the Ph.D. degree in biological and health sciences from the University of Bordeaux, France, in 1998. She is currently a CNRS Research Engineer with the IMS Laboratory. She is the Head of the Life Platform dedicated to implementation of original biological methodologies at the interface of physics and electronics. The platform's activities focus on the harmful and beneficial biological effects of electromagnetic fields and on the proposal of cellular or animal models adapted to bioelectronic sensors. She has been an Elected Board Member of BioEM Council, since 2020. She is the author of forty peer-reviewed articles, and more than 100 conference publications.

ANTOINE PIROG received the Engineering degree and the M.Sc. degree in electronics engineering from ENSEIRB-MATMECA (FR), in 2014, and the Ph.D. degree in electronics from the University of Bordeaux, in 2017. He is currently an Associate Professor in electronics at JUNIA and IMS UMR5218, University of Bordeaux, in the Bioelectronics Group and the Innovative Technologies for Healthcare Team. His research interests include pluridisciplinary topics such as electronic devices for the acquisition and processing of electrophysiological signals, biological cell-based biosensors, closed-loop cell-hardware hybrid systems for the artificial pancreas, and bio-inspired algorithms.

GILLES N'KAOUA received the Engineering degree in electronics engineering from CNAM, Paris, France, in 1992. He is currently a Research Engineer with CNRS (National Council of Scientific Research) and IMS UMR5218 (Talence, France). From 1993 to 2008, he was in charge of IMS clean rooms for microtechnology designs. He joined the BioElectronics Research Group in IMS, in 2008. In the group, he is an in charge of the development and support of instruments and embedded systems. Since 2017, he has also been the National Coordinator of the CNRS Professional Network of Electronic Engineers and Technicians.

ADRIEN D'HOLLANDE received the Engineering degree and the M.Sc. degree in electronics engineering from ENSEIRB-MATMECA (France), in 2021. He is currently pursuing the M.Sc. degree in biomedical engineering science with Université Paris Sciences et Lettres (PSL) and Université Paris Cité, Paris, (France). He was with the IMS laboratory at Bordeaux (France).

AURELIAN HOUE received the Engineering degree and the M.Sc. degree in electronics engineering from ENSEIRB-MATMECA, France, in 2021. He is currently pursuing the Ph.D. degree in engineering science with the LABSTICC, CNRS UMR 6285 in Brest (France). He was with the IMS laboratory at Bordeaux (France).

FABIEN SOULIER received the Engineer Diploma degree in electrical engineering and the M.Sc. degree in signal processing from the Grenoble Institute of Technology, France, in 1998. He got the rank of "Prof. Agrégé" in applied physics, in 1999, and the Ph.D. degree from the University of Poitiers, France, in 2003.

He is currently an Associate Professor with the École Polytechnique Universitaire de Montpellier, and a member of the Microelectronic Integrated System Department of the Laboratoire d'informatique, de robotique et de microélectronique de Montpellier (LIRMM), University of Montpellier, France. He has participated to the supervision of nine Ph.D., authored or coauthored 46 international journal and conference papers, and contributed to the redaction of two book chapters. His research interests include the analog and mixed design of bioelectronic circuits and systems, biosignal processing, bioimpedance spectroscopy, embedded environmental sensors, and biosensors.

SERGE BERNARD received the M.S. degree in electrical engineering from the University of Paris XI, France, in 1998, and the Ph.D. degree in electrical engineering from the University of Montpellier, France, in 2001.

He was the Director of the joint Institute for System Testing ISyTest between the LIRMM and NXP semiconductors. He was the Head of the Laboratory of Computer Science, Robotics and Microelectronics of Montpellier, Microelectronics Department. He is currently a Researcher of the National Council of Scientific Research (CNRS), LIRMM, Microelectronics Department. He has participated to the supervision of 17 Ph.D., contributed to three patents, authored or coauthored over 110 international papers, and contributed to the redaction of two books on these topics. His main research interests include test, design-for-testability and built-in-self-test for mixed-signal circuits and SiP, and design-for-reliability for medical application ICs.

Dr. Bernard was the General Chair of the 27th Conference on Design of Circuits and Integrated Systems (DCIS) and the 21st International Mixed-Signal Testing Workshop (IMSTW). He was the Program Chair of two international conferences (DDECS'14 and DTIS'12). He has been involved in ten European research projects as participant or he is the Project Leader of one of them (FISHNCHIP).

SYLVIE RENAUD received the Engineer Diploma and M.Sc. degrees in electronic engineering from SUPELEC, Paris, France, in 1986, and the Ph.D. degree in engineering from University of Bordeaux, France, in 1990.

She is currently a Professor in electronics with the Bordeaux Institute of Technology and IMS UMR5218, a joint research unit between CNRS, University of Bordeaux and Bordeaux INP (France). She conducts research in bioelectronics, where she integrates IC design and biomedical technological needs in an interdisciplinary approach. She participated or coordinated 14 international and national research projects and authored more than 50 reviewed international articles and communications. Her research interests include analog and mixed neuromorphic VLSI, hardware platforms of real-time spiking neural networks, hybrid systems interfacing living and artificial neurons, analog ASICs for biological signal conditioning and events detection, active VLSI implants for neurodegenerative diseases and diabetes, and closed-loop living-artificial systems for clinical-driven applications.

Dr. Renaud was appointed as a member of the CNRS Engineering Department (INSIS) Scientific Council, from 2015 to 2019. In 2021, she was nominated as a Board Member for the Micro-Nanotechnologies Section 08 of the National Committee for Scientific Research (CoNRS). She was an Associate Editor for the IEEE TRANSACTIONS ON BIOMEDICAL CIRCUITS AND SYSTEMS journal, and the Deputy Director of IMS (2016–2021).